Plant Hydraulic Transport Controls Transpiration Response to Soil Water Stress

Brandon P. Sloan[1,2], Sally E. Thompson[3], and Xue Feng[1,2]

[1]Department of Civil Environmental and Geo-Engineering, University of Minnesota - Twin Cities, Minneapolis, MN 55455
[2]Saint Anthony Falls Laboratory, University of Minnesota - Twin Cities, Minneapolis, MN 55455
[3]Department of Civil, Environmental and Mining Engineering, University of Western Australia, Perth, Australia

Correspondence: Brandon Sloan (sloan091@umn.edu)

Abstract. Plant transpiration downregulation in the presence of soil water stress is a critical mechanism for predicting global water, carbon, and energy cycles. Currently, many terrestrial biosphere models (TBMs) represent this mechanism with an empirical correction function (β) of soil moisture—a convenient approach that can produce large prediction uncertainties. To reduce this uncertainty, TBMs have increasingly incorporated physically-based Plant Hydraulic Models (PHMs). However, PHMs introduce additional parameter uncertainty and computational demands. Therefore, understanding why and when PHM and β predictions diverge would usefully inform model selection within TBMs. Here, we use a minimalist PHM to demonstrate that coupling the effects of soil water stress and atmospheric moisture demand leads to a spectrum of transpiration response controlled by soil-plant hydraulic transport (conductance). Within this transport-limitation spectrum, β emerges as an end-member scenario of PHMs with infinite conductance, completely decoupling the effects of soil water stress and atmospheric moisture demand on transpiration. As a result, PHM and β transpiration predictions diverge most when conductance is low (transport-limited), atmospheric moisture demand variation is high, and soil moisture is moderately available to plants. We apply these minimalist model results to land surface modeling of an Ameriflux site. At this transport-limited site, a PHM downregulation scheme outperforms the β scheme due to its sensitivity to variations in atmospheric moisture demand. Based on this observation, we develop a new 'dynamic β' that varies with atmospheric moisture demand—an approach that balances realism with parsimony and overcomes existing biases within β schemes.

1 Introduction

Plants control their water use (i.e., transpiration (T)) and CO_2 assimilation by adjusting leaf stomatal apertures in response to environmental variations (Katul et al., 2012; Fatichi et al., 2016). In doing so, they mediate the global water, carbon, and energy cycles. The performance of most terrestrial biosphere models (TBMs) relies on accurately representing leaf stomatal responses in terms of stomatal conductance (g_s). Extensive research has established the relationships between g_s and atmospheric conditions like photosynthetically active radiation, humidity, CO_2 concentration, and air/leaf temperature (see Buckley and Mott (2013) and references therein) under well-watered conditions, though the specific forms of these relationships vary (Damour et al., 2010). However, representing the dynamics of g_s in response to soil water stress remains problematic.

Many TBMs represent declining g_s and, in turn, transpiration reduction (i.e., downregulation) in response to soil water stress

25 with an empirical function of soil water availability. This method, known as β (Powell et al., 2013; Verhoef and Egea, 2014; Trugman et al., 2018; Paschalis et al., 2020), reduces transpiration from its peak value under well-watered conditions (T_{ww}), i.e., $T = \beta \cdot T_{ww}, 0 \leq \beta \leq 1$. (We use the term '$\beta$' in this paper to refer to the downregulation model itself, and the terms 'β function' or 'β factor' to refer to the empirical function and its values, respectively.) β originated as a heuristic assumption when modeling flow around roots in soils (Feddes et al., 1978) and gained widespread use within TBMs and hydrological

30 models due to its parsimonious form.

However, mounting evidence indicates that using β in TBMs is a major source of uncertainty and bias in plant-mediated carbon and water flux predictions. Multiple studies have implicated the lack of a universal β formulation as a primary source of intermodel variability in carbon cycle predictions (Medlyn et al., 2016; Rogers et al., 2017; Trugman et al., 2018; Paschalis et al., 2020). For example, different β formulations among nine TBMs were responsible for 40%-80% of intermodel variability

35 in global gross primary productivity (GPP) predictions (on the order of 3-283% of current GPP) (Trugman et al., 2018). Aside from the uncertainty in functional form, β appears to fundamentally misrepresent the coupled effects of soil water stress and atmospheric moisture demand on stomatal closure. Recent work using model-data fusion at FLUXNET sites highlighted that β is overly sensitive to soil water stress and unrealistically insensitive to atmospheric moisture demand (Liu et al., 2020). Furthermore, TBM validation experiments have found β schemes produce unrealistic GPP prediction during drought at Amazon

40 rainforest sites (Powell et al., 2013; Restrepo-Coupe et al., 2017) and systematic overprediction of evaporative drought duration, magnitude and intensity (Ukkola et al., 2017) at several Ameriflux sites. The apparent inadequacy of β has lead to the adoption of physically-based Plant Hydraulic Models (PHMs) in TBMs (Williams et al., 2001; Bonan et al., 2014; Xu et al., 2016; Kennedy et al., 2019; Eller et al., 2020; Sabot et al., 2020).

PHMs represent water transport through the soil-plant-atmosphere continuum via flux-gradient relationships (based on

45 Hagen-Poiseuille flow) and conductance curves (Mencuccini et al., 2019). The implementation of PHMs in several popular TBMs (e.g., CLM, JULES, etc.) has improved predictions in site-specific GPP and evapotranspiration (ET) predictions (Powell et al., 2013; Bonan et al., 2014; Eller et al., 2020; Sabot et al., 2020; Kennedy et al., 2019) as well as soil water dynamics (Kennedy et al., 2019) compared to β. PHMs also exhibit more realistic sensitivity to atmospheric moisture demand than β (Liu et al., 2020). However, these improvements from PHMs come at the cost of an increased number of plant hydraulic trait

50 parameters and computational burden, which can reduce the robustness and reliability of the predictions (Prentice et al., 2015). Additionally, plant hydraulic traits are difficult to constrain: they vary widely across and within species (Anderegg, 2015) and exhibit plasticity through adaptation. Furthermore, the traits are measured at stem, branch or leaf levels, and scaling them to represent stand or ecosystem behavior remains challenging (Feng, 2020). Consequently, modelers continue to rely on β as a parsimonious alternative to PHMs (Paschalis et al., 2020).

55 The relative strengths and weaknesses of β and PHMs suggest that informed model selection requires a better understanding of when the complexity of a PHM is justified over the simplicity of β. This paper informs such understanding by: i) analyzing the fundamental differences between PHMs and β and their controlling parameters (Sect. 3.1-3.2), ii) demonstrating the environmental conditions where PHMs outperform β (Sect. 3.2-3.3), and iii) leveraging our theoretical insights to create a

new 'dynamic β' that captures the realism of PHMs while retaining the simplicity of the original β (Sect. 3.3). To do this,
we first analyze a minimalist PHM using a supply-demand framework, then corroborate the results using a more widely-used,
complex PHM, and finally perform a case study with a calibrated land surface model (LSM) using β, PHM, and 'dynamic β'
downregulation schemes.

2 Methods

2.1 Minimalist PHM

Our minimalist PHM analysis (Sect. 3.1-3.2) uses a supply-demand framework that conceptualizes transpiration as the joint out-
come of soil water supply and atmospheric moisture demand (Gardner, 1960; Cowan, 1965; Sperry and Love, 2015; Kennedy
et al., 2019). In this framework, 'supply' refers to the rate of water transport to the leaf mesophyll cells from the soil, into the
roots, and through the xylem. 'Demand' refers to the rate of water vapor outflux through the stomata, regulated by stomatal
response to atmospheric conditions (Buckley and Mott, 2013) and leaf water potential (Jarvis, 1976; Sperry et al., 1998; Klein,
2014; McAdam and Brodribb, 2016; Anderegg et al., 2017) and driven by the transport capacity of the air surrounding the
plant.

The minimalist PHM supply (T_s^{phm} [W m^{-2}]; Eq. 1) is represented by an integrated 1-D flux-gradient relationship, bounded
by soil and leaf water potentials (ψ_s and ψ_l [MPa]) and mediated by the bulk conductance along the flowpath ($g_{sp}(\psi)$
[W m^{-2} MPa^{-1}]). Following Manzoni et al. (2014), we assume constant soil-plant conductance (g_{sp}) and steady state transpi-
ration to simplify the integral in Eq. 1 to the product of soil-plant conductance and water potential difference from soil to leaf.
The minimalist PHM demand (T_d^{phm} [W m^{-2}]; Eq. 2) consists of a downregulation function ($f(\psi_l)$) multiplied by the well-
watered transpiration rate (T_{ww} [W m^{-2}]). $f(\psi_l)$ represents stomatal closure under low ψ_l (Jarvis, 1976; Klein, 2014) and can
take a piecewise linear form (Eq. 3) parametrized by the leaf water potential at incipient ($\psi_{l,o}$) and complete stomatal closure
($\psi_{l,c}$). T_{ww} is the product of well-watered stomatal conductance ($g_{s,ww}$ [W m^{-2} MPa^{-1}]) and the vapor pressure deficit (D
[MPa]). For clarity, 'well-watered' refers to abundant soil water conditions under which water transport to the leaves maintains
ψ_l high enough to avoid stomatal closure; therefore, T_{ww} and $g_{s,ww}$ only depend on atmospheric conditions. In the minimalist
analysis, T_{ww} values were selected and not calculated.

$$T_s^{phm} = -\int_{\psi_s}^{\psi_l} \frac{K_p(\psi)\, d\psi}{z_{\psi_l} - z_{\psi_s}} = -\int_{\psi_s}^{\psi_l} g_{sp}(\psi)\, d\psi = g_{sp} \cdot (\psi_s - \psi_l) \tag{1}$$

$$T_d^{phm} = f(\psi_l) \cdot g_{s,ww} \cdot D = f(\psi_l) \cdot T_{ww} \tag{2}$$

85 $$f\left(\psi_l\right) = \begin{cases} 1 & \psi_l \geq \psi_{l,o} \\ \frac{\psi_{l,c}-\psi_l}{\psi_{l,c}-\psi_{l,o}} & \psi_{l,c} < \psi_l < \psi_{l,o} \\ 0 & \psi_l \leq \psi_{l,c} \end{cases}$$ (3)

The steady state transpiration rate for the minimalist PHM (T^{phm}; Eq. 4) is found at the leaf water potential where supply equals demand (ψ_l^*). The equation for ψ_l^* is derived by equating Eq. 1-2 and solving for ψ_l (Eq. 5). Equation 5 is substituted into Eq. 1 to yield T^{phm} (Eq. 4). The full derivation is shown in section S1 of the Supplement.

$$T^{phm} = \begin{cases} T_{ww} & \psi_s > \psi_{l,o} + \frac{T_{ww}}{g_{sp}} \\ T_{ww} \cdot \frac{(\psi_{l,c}-\psi_s)}{(\psi_{l,c}-\psi_{l,o})-\frac{T_{ww}}{g_{sp}}} & \psi_{l,c} < \psi_s \leq \psi_{l,o} + \frac{T_{ww}}{g_{sp}} \\ 0 & \psi_s \leq \psi_{l,c} \end{cases}$$ (4)

90 $$\psi_l^* = \frac{\psi_s \cdot (\psi_o - \psi_c) + \frac{T_{ww} \cdot \psi_c}{g_{sp}}}{(\psi_o - \psi_c) + \frac{T_{ww}}{g_{sp}}}$$ (5)

2.2 Complex PHM

The LSM analysis in this paper (Sect. 3.3) uses a more complex PHM formulation following Feng et al. (2018). The PHM segments supply into soil-to-xylem and xylem-to-leaf compartments and demand into a leaf-to-atmosphere compartment. The conductance in each compartment consists of a maximum conductance downregulated by a function of water potential. In the supply compartments, the dependence of conductance on water potential represents 'hydraulic limits' (Sperry et al., 1998) that arise via (i) the inability of roots to remove water from soil pores at low ψ_s and (ii) xylem embolism caused by large hydraulic gradients required under low ψ_s and/or high T_{ww}. The soil-to-xylem conductance (g_{sx} [W m^{-2} MPa^{-1}]; Eq. 6) is its maximum value ($g_{sx,max}$) downregulated by the unsaturated soil hydraulic conductivity curve (Clapp and Hornberger, 1978) which is parametrized by the saturated soil water potential (ψ_{sat}), soil water retention exponent (b), unsaturated hydraulic conductivity exponent ($c = 2b+3$), and a correction factor ($d = 4$) to account for roots' ability to reach water (Daly et al., 2004). The xylem-to-leaf conductance (g_{xl} [W m^{-2} MPa^{-1}]; Eq. 7) is its maximum value ($g_{xl,max}$) downregulated by a sigmoidal function (Pammenter and Willigen, 1998) which is parametrized by the vulnerability exponent (a) and the xylem water potential (ψ_x) at 50% loss of conductance ($\psi_{x,50}$). The $g_{sx,max}$ and $g_{xl,max}$ values are estimated using trait-based equations following Feng et al. (2018) (see section S6 of the Supplement).

105 $$g_{sx}\left(\psi\right) = g_{sx,max} \cdot \left(\frac{\psi_{sat}}{\psi}\right)^{\frac{c-d}{b}}$$ (6)

$$g_{xl}(\psi) = g_{xl,max} \cdot \left[1 - \frac{1}{e^{a(\psi - \psi_{x,50})}} \right] \tag{7}$$

The single demand compartment represents leaf-to-atmosphere conductance (Eq. 8) as the stomatal conductance (g_s; Eq. 8) downregulated from its well-watered value ($g_{s,ww}$) using a Weibull function which is parmetrized by a shape factor (b_l) describing stomatal sensitivity and the leaf water potential at 50% loss of conductance ($\psi_{l,50}$) (Klein, 2014). This Weibull

110 form is similar to the piecewise linear form of $f(\psi_l)$ in the minimalist PHM (Eq. 3), but is more consistent with formulations common in TBMs (Oleson et al., 2018). The $g_{s,ww}$ value (Eq. 9) is estimated by the Medlyn optimal stomatal conductance model (Medlyn et al., 2011) which is parametrized by the minimum stomatal conductance (g_o [$\mathrm{mol\,H_2O\,m^{-2}\,s^{-1}}$]), Medlyn slope parameter (g_1 [$\mathrm{Pa^{0.5}}$]), vapor pressure deficit (D [Pa]), net CO_2 assimilation rate (A_n [$\mathrm{mol\,CO_2\,m^{-2}\,s^{-1}}$]), partial pressure of CO_2 at the leaf surface (c_s [Pa]), and atmospheric pressure (P_{atm} [Pa]). We refer the reader to section S6 and S7

115 of the Supplement for full details and parameter values.

$$g_s = g_{s,ww} \cdot e^{-\left(\frac{\psi_l}{\psi_{l,50}}\right)^{b_l}} \tag{8}$$

$$g_{s,ww} = g_o + \left(1 + \frac{g_1}{\sqrt{D}} \right) \cdot \frac{1.6 \cdot A_n}{c_s / P_{atm}} \tag{9}$$

The steady-state solution of the complex PHM requires finding the leaf (ψ_l^*) and xylem water potential (ψ_x^*) that balance transport in the three compartments. To calculate supply in each compartment ($T_{s,sx}$ and $T_{s,xl}$), we use a Kirchhoff transform to

120 account for conductance varying with water potential along the flow path (Eq. 10) (Sperry et al., 1998) and take the difference in the matric flux potential (Φ) at the segment endpoints (Eq. 11-12). The demand (T_d; Eq. 13) is the stomatal conductance scaled by leaf area index (LAI) and multiplied by D. The values of ψ_l^* and ψ_x^* that balance flow in each compartment are found using nonlinear least squares. The single big-leaf formulation outlined here has been extended to a two-big leaf formulation used in the LSM analysis (see section S6 of the Supplement for full details). Equations 11-13 contain constants for the latent

125 heat of vaporization ($\mathcal{L}_v$ [$\mathrm{J\,kg^{-1}}$]), density of water (ρ_w [$\mathrm{kg\,m^{-3}}$]), density of air (ρ_a [$\mathrm{kg\,m^{-3}}$]), molar density of an ideal gas (ρ_m [$\mathrm{mol\,m^{-3}}$]), and the ratio of molar weight of water to air (ε) to convert transpiration fluxes to units of $\mathrm{W\,m^{-2}}$.

$$\Phi(\psi) = \int_{-\infty}^{\psi} g(\psi')\, d\psi' \tag{10}$$

$$T_{s,sx} = [\Phi_{sx}(\psi_s) - \Phi_{sx}(\psi_x)] \cdot \rho_w \cdot \mathcal{L}_v \tag{11}$$

$$T_{s,xl} = [\Phi_{xl}(\psi_x) - \Phi_{xl}(\psi_l)] \cdot \rho_w \cdot \mathcal{L}_v \tag{12}$$

$$T_d = LAI \cdot g_s \cdot D \cdot \frac{\mathcal{L}_v \cdot \rho_a \cdot \rho_m \cdot \varepsilon}{P_{atm}} \qquad (13)$$

130

2.3 LSM Description and Calibration

The LSM created for this work (Sect. 3.3) is a dual-source, 2-big leaf approximation (Bonan, 2019) adapted from CLM v5 (Oleson et al., 2018) with several key simplifications: 1) steady-state conditions, 2) negligible atmospheric stability, 3) use of the Goudriaan and van Laar radiative transfer model (Goudriaan and Laar, 1994), and 4) forced with soil moisture, soil heat

135 flux and radiative forcing data. Our simplified LSM allowed parallel computation and removal of confounding model structural errors. We refer the reader to section S6 of the Supplement for full model details and justifications. The model was formulated in MATLAB and codes will be made available online with acceptance of this manuscript.

We ran five separate LSMs for this analysis, each with a different transpiration downregulation scheme: 1) well-watered (no downregulation), 2) a single β (β_s) with static parameters, 3) a β separately applied to sunlit and shaded leaf areas (β_{2L})

140 with static parameters, 4) a 'dynamic β' with parameters dependent on T_{ww} (β_{dyn}), and 5) a PHM. We calibrated the LSM with PHM downregulation scheme by simulating 13,600 parameter sets using Progressive Latin Hypercube Sampling (Razavi et al., 2019) on 15 selected soil and plant parameters. The best parameter set was selected by comparison of RMSE, correlation coefficient, percent bias and variance with Ameriflux evapotranspiration, sensible heat flux, gross primary productivity, and net radiation site data. We provide full calibration details in section S5 of the Supplement.

145 We fit the three LSMs with β schemes to the relative transpiration outputs (T/T_{ww}) of the calibrated LSM, while the well-watered LSM was run with the calibrated parameters and downregulation turned off. The choice to calibrate a single LSM ensured that the performance differences between the schemes would be due to the PHM representing plant water use more realistically and not to the artifact of differing parameter fits between models. We refer the reader to section S2.2 of the Supplement for specific details of the parameter fits for the β schemes.

2.4 Site Description

150

We selected the US-Me2 "Metolius" Ameriflux site (Irvine et al., 2008) for our modeling case study due to its comprehensive atmospheric and subsurface data availability. The site consists of intermediate-age ponderosa pine on sandy loam soil in the Metolius River Basin in Oregon, USA. Previous modeling (Schwarz et al., 2004) and measured soil parameters and hydraulic traits (Irvine et al., 2008) helped guide calibration. Volumetric soil water content and soil temperature measurements over

155 multiple depths and years enabled the model results to be tested against the selection of different soil moisture depths to represent plant water availability. Full description of the forcing data is given in section S4 of the Supplement.

2.5 β Formulations

As mentioned previously, the β transpiration downregulation model does not have a universal formulation. β functions have been heuristically defined using a variety of water supply proxies including ψ_l (Jarvis, 1976), ψ_s (Verhoef and Egea, 2014),

160 and volumetric soil water content (θ_s) (Verhoef and Egea, 2014). Additionally, once the β function is selected, the choice remains of where to apply the β factor; some TBMs apply the β factor directly to T_{ww}, whereas others apply it to parameters that control T_{ww}, like $g_{s,ww}$ (Kowalczyk et al., 2006) or maximum photosynthetic rates (Zhou et al., 2013; Lin et al., 2018; Kennedy et al., 2019). Here, we have elected to define the β function in terms of ψ_s and apply the β factor directly to T_{ww} (Eq. 14) as it mirrors the PHM demand equations. In the minimalist analysis (Sect. 3.1-3.2), $\beta(\psi_s)$ (Eq. 15) takes a piecewise linear

165 form (analogous to Eq. 3) which is parametrized by the soil water potential at incipient ($\psi_{s,o}$) and complete stomatal closure ($\psi_{s,c}$). Similarly, in the LSM analysis (Sect. 3.3), $\beta(\psi_s)$ (Eq. 16) takes a Weibull form (analogous to Eq. 8) parametrized by the soil water potential at 50% loss of stomatal conductance ($\psi_{s,50}$) and a stomatal sensitivity parameter (b_s). The LSM analysis uses two versions of Equation 16: 1) a static version with constant b_s and $\psi_{s,50}$ (used by the β_s and β_{2L} schemes), and 2) a dynamic version where b_s and $\psi_{s,50}$ are linear functions of T_{ww} (used by the β_{dyn} scheme).

170 $$T^\beta = \beta(\psi_s) \cdot T_{ww} \tag{14}$$

$$\beta(\psi_s) = \begin{cases} 1 & \psi_s \geq \psi_{s,o} \\ \frac{\psi_{s,c} - \psi_s}{\psi_{s,c} - \psi_{s,o}} & \psi_{s,c} < \psi_s < \psi_{s,o} \\ 0 & \psi_s \leq \psi_{s,c} \end{cases} \tag{15}$$

$$\beta(\psi_s, T_{ww}) = e^{-\left(\frac{\psi_s}{\psi_{s,50}(T_{ww})}\right)^{b_s(T_{ww})}} \tag{16}$$

3 Results

3.1 β as a Limiting Case of PHMs with Infinite Conductance

175 Looking at the minimalist PHM and β models in a supply-demand framework reveals their fundamental differences. The PHM supply lines (red lines in Fig. 1a) illustrate water transport from soil-to-leaf (Eq. 1) at fixed soil water availability (ψ_s) with increasing pull from the leaf (lower ψ_l). The PHM demand lines (black lines in Fig. 1a) illustrate transpiration rate decline (due to stomatal closure) with lower ψ_l for two atmospheric moisture demands, represented by the well-watered transpiration rate (T_{ww}). The intersection of the supply and demand lines in Fig. 1a is the minimalist PHM solution (T^{phm}; Eq. 4) at the leaf

180 water potential (ψ_l^*; Eq. 5) that equates supply with demand. The difference between ψ_s and ψ_l^* is the water potential difference ($\Delta\psi$) that drives flow through the soil-plant system mediated by the soil-plant conductance (g_{sp} and slope of supply lines). The minimalist PHM couples the effects of soil water stress to atmospheric moisture demand on transpiration downregulation because leaf water potential (ψ_l^*) responds to both ψ_s and T_{ww} until the equilibrium transpiration is reached. The empirical β does not readily map to our supply-demand framework since the β function is a lumped representation of the soil-plant system.
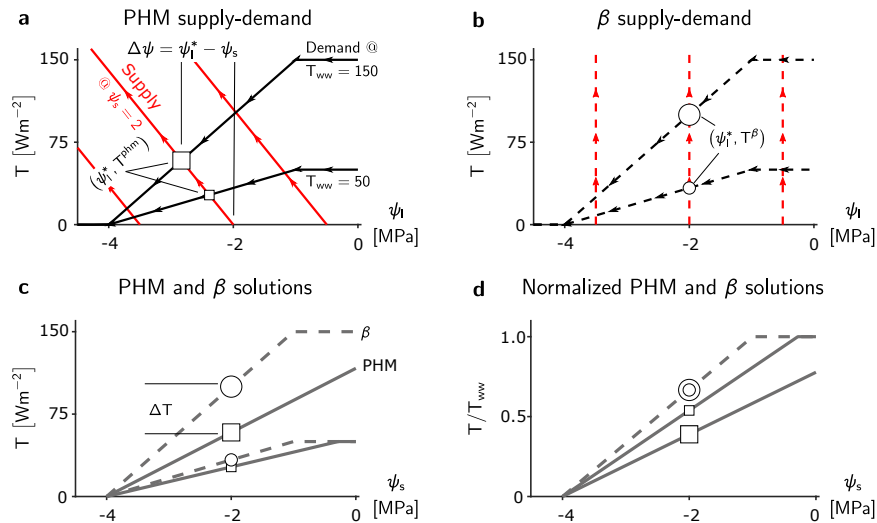
Figure 1. Fundamental differences between minimalist PHM and β. **a-b,** Supply (red) and demand (black) curves for PHM (**a**, solid lines) and β (**b**, dashed lines) under varying leaf water potentials (ψ_l). The squares (circles) represent the PHM (β) solution — i.e., the ψ_l^* where supply equals demand — for a single soil water availability (ψ_s) and two atmospheric moisture demands (T_{ww}). These markers carry through panels **c** and **d** to illustrate how the solutions between the PHM and β diverge at a single ψ_s. The relative size of the markers indicates corresponding T_{ww}. The water potential difference $\Delta\psi$ required to transport water from soil to leaf is shown in panel **a** for $\psi_s = -2$ MPa and $T_{ww} = 150$ W m^{-2}. **c,** Solutions of panels **a** and **b** mapped to ψ_s, where ΔT is the difference between PHM and β transpiration estimates at $\psi_s = -2$ MPa and $T_{ww} = 150$ W m^{-2}. **d,** Relative transpiration, in which solutions in panel **c** are normalized by T_{ww}. The β solutions collapse to a single curve, whereas the PHM solutions depend on T_{ww}.

185   However, the β transpiration rate (T^β, Eq. 14) decouples the effects of soil water stress and atmospheric moisture demand on downregulation: the β function depends only on soil water availability, and T_{ww} depends only on atmospheric conditions.

The coupling inherent to the PHM results in greater transpiration downregulation compared to β under the same environmental conditions (Fig. 1c). β downregulates transpiration at a fixed proportion based on ψ_s only (i.e., it scales linearly with T_{ww}); hence, it can be modeled with a single curve (Fig. 1d). Unlike β, the PHM downregulates transpiration at a greater

190   proportion with increasing atmospheric moisture demand (i.e., it scales nonlinearly with T_{ww}), and thus must be described as a function of both ψ_s and T_{ww}. Physically, this result stems from a larger water potential difference ($\Delta\psi = \psi_s - \psi_l^*$), and thus a lower ψ_l, required for transport through the soil-plant system under higher atmospheric moisture demand, resulting in greater stomatal closure and thus further downregulation (i.e., smaller transpiration relative to T_{ww} in Fig. 1d).

The physical conditions leading to the empirical β assumptions result from supply-demand curves that independently ac-

195   count for the effects of soil water stress and atmospheric moisture demand on transpiration downregulation. This situation only arises when the supply lines are vertical (Fig. 1b), resulting in $\psi_l^* = \psi_s$ and the relative transpiration (T^β/T_{ww}) collapsing to a single curve (Fig. 1d). Since g_{sp} represents the supply line slope (Eq. 1), β is revealed as a limiting case of the PHM in which the soil-plant system is infinitely conductive. We can formally show this limiting behavior in Eq. 17 and 18, where ψ_s

approaches ψ_l^* and the difference in PHM and β solutions (ΔT) approaches 0 as $g_{sp} \to \infty$. Interpreted this way, the $\beta(\psi_s)$
function (Eq. 15) represents stomatal closure to declining leaf water potential because of its equivalence to $f(\psi_l)$ (Eq. 3) in
PHMs. Therefore, a physical interpretation of β is transpiration downregulation due purely to stomatal closure as leaf water
potentials decline, occurring in an infinitely conductive soil-plant system that causes water potential to remain unchanged
between soil and leaf.

$$
\lim_{g_{sp} \to \infty} [\psi_l^*] = \lim_{g_{sp} \to \infty} \left(\frac{\psi_s \cdot (\psi_o - \psi_c) + \frac{T_{ww} \cdot \psi_c}{g_{sp}}}{(\psi_o - \psi_c) + \frac{T_{ww}}{g_{sp}}} \right) = \psi_s \tag{17}
$$

$$
\lim_{g_{sp} \to \infty} (\Delta T) = \lim_{g_{sp} \to \infty} \left(T^{phm} - T^\beta \right) = \lim_{g_{sp} \to \infty} \left(T_{ww} \cdot \left[\frac{(\psi_{l,c} - \psi_s)}{(\psi_{l,c} - \psi_{l,o}) - \frac{T_{ww}}{g_{sp}}} - \frac{(\psi_{l,c} - \psi_s)}{(\psi_{l,c} - \psi_{l,o})} \right] \right) = 0 \tag{18}
$$

These minimalist model results suggest that the range of soil-plant conductances (g_{sp}) can generate a spectrum of possible
transpiration responses to soil water stress. Two classes of behaviors emerge—one in a 'supply-limited' soil-plant system,
in which g_{sp} is large enough for $\psi_l \approx \psi_s$, thus decoupling the effects of soil water stress and atmospheric moisture demand
while allowing the relative transpiration to vary only with ψ_s (Fig. 1d). The other class of behavior arises in 'transport-limited'
systems with finite g_{sp}, in which a non-negligible water potential difference ($\Delta \psi$) is required to transport the water to the
leaf, resulting in additional downregulation compared to supply-limited systems (Fig. 1d) and requiring relative transpiration
to depend on both ψ_s and T_{ww}.

3.2 Parameters Controlling the Divergence of β and PHMs

The differences in PHM and β transpiration estimates (ΔT) depends not only on g_{sp}, but also on soil water availability (ψ_s),
atmospheric moisture demand (T_{ww}) and plant water use strategy ($\psi_{l,c} - \psi_{l,o}$) (Fig. 2). Changes in ψ_s are represented by the
translation of the supply lines (Fig. 2a,c,e) and result in non-monotonic behaviors in ΔT over the range of soil water stress
($\psi_{l,c} < \psi_s < \psi_{l,o} + T_{ww}/g_{sp}$) (Fig. 2b,d,f). The peak ΔT occurs at the incipient point of stomatal closure ($\psi_{l,o}$) because i)
when $\psi_s < \psi_{l,o}$, transpiration begins to decrease, and in its extreme limit, transpiration (and thus ΔT) approaches 0 and ii)
when $\psi_s > \psi_{l,o}$, the effects of downregulation diminish in both models.

The ΔT-ψ_s non-monotonic behavior inversely scales with g_{sp}, as decreasing the soil-plant conductance (and thus increasing
transport-limitation) results in flatter supply lines and greater $\Delta \psi$ (Fig. 2a). Furthermore, the range of ψ_s with higher ΔT
increases due to increase in the range of soil water stress for the PHM. The ΔT-ψ_s behavior also scales with atmospheric
moisture demand (Fig. 2d) as greater demand line slope results in greater $\Delta \psi$ (Fig. 2c). Lastly, the plant water use strategy
($\psi_{l,c} - \psi_{l,o}$) approximates how sensitive stomatal closure is to ψ_l. A more aggressive strategy—closing stomata over a narrower
range of ψ_l and ψ_s—increases ΔT as the demand lines becomes more vertical (Fig. 2e). However, this results in a narrower
range of soil water stress meaning periods of significant ΔT may occur infrequently (Fig. 2f). In summary, this analysis
suggests that PHMs are most needed to represent transport-limited soil-plant systems under high atmospheric moisture demand
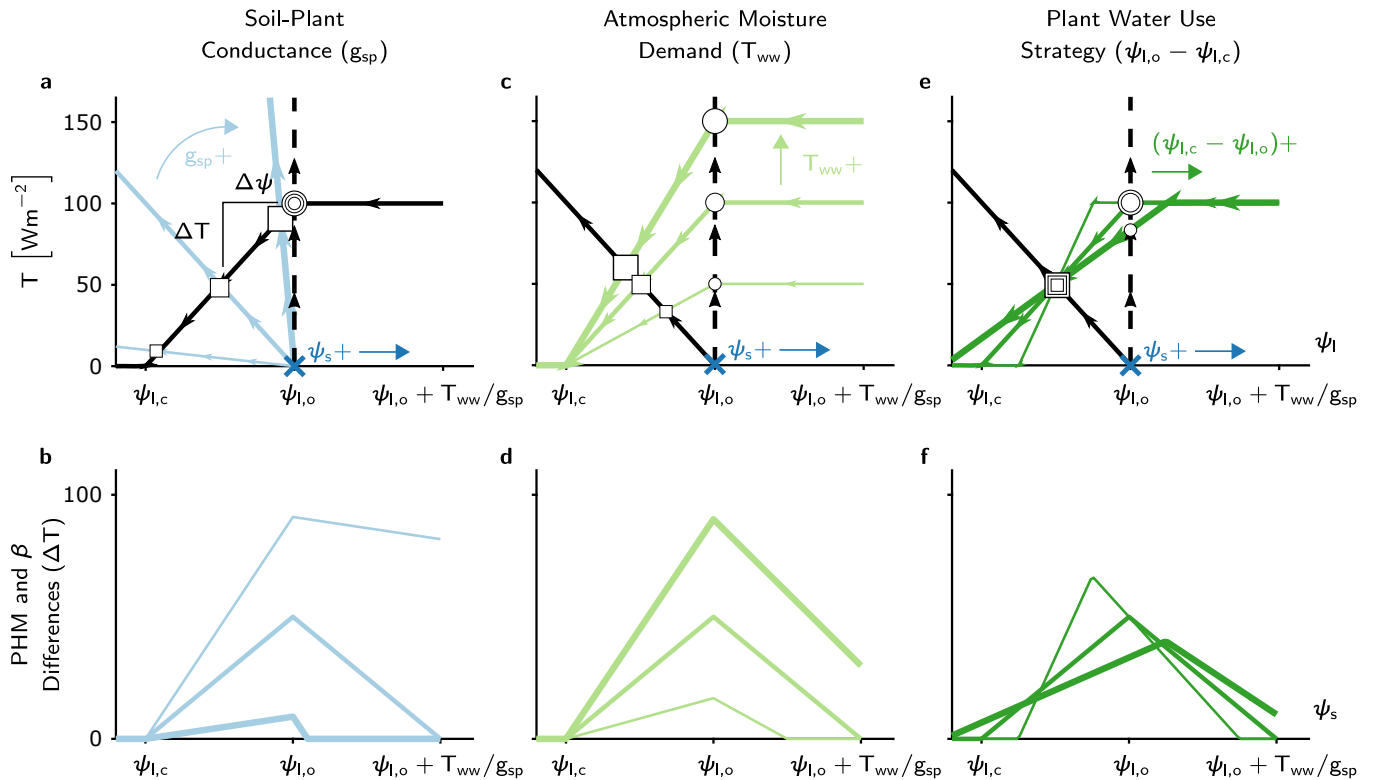
Figure 2. The effect of soil water potential (ψ_s), soil-plant conductance (g_{sp}), atmospheric moisture demand (T_{ww}) and plant water use strategy ($\psi_{l,o} - \psi_{l,c}$) on differences between the minimalist PHM and β models (ΔT). **a,c,e,** Supply-demand curves at a single soil water availability (indicated by the dark blue x at $\psi_s = \psi_{l,o}$), for three prescribed values of g_{sp}, T_{ww}, and $\psi_{l,o} - \psi_{l,c}$, respectively. Each parameter (g_{sp}, T_{ww}, or $\psi_{l,o} - \psi_{l,c}$) is set at 50% above (below) its base values at $g_{sp} = 100\,\mathrm{W\,m^{-2}\,MPa^{-1}}$, $T_{ww} = 75\,\mathrm{W\,m^{-2}}$, $\psi_o = -1\,\mathrm{MPa}$, and $\psi_o = -2\,\mathrm{MPa}$ using thick (thin) colored lines. The squares (circles) indicate the PHM (β) solutions, with size corresponding to magnitude of the changing parameter values. Note: the vertical distance between correspondingly sized circle and square is ΔT and horizontal distance is $\Delta\psi$. **b,d,f,** The ΔT results from the panels **a**, **c**, and **e** calculated for a range of ψ_s with line thickness proportional to parameters in the aforementioned panels (e.g., thick blue line in panel **b** corresponds to 50% increase in g_{sp} shown in panel **a**). The x-axes are mapped from ψ_l in the top panels to ψ_s in the bottom panels.

variability and moderate soil water stress, especially if downregulation occurs abruptly as a function of soil water stress. The
230 reason PHMs are needed for high atmospheric moisture demand variability is that β is empirical and could be fit to observations
at differing T_{ww} values. We discuss this point more thoroughly in the Sect. 3.3.

3.3 Improving Transpiration Predictions with a PHM and a 'Dynamic β'

We now examine the divergence between PHMs and β for a real transport-limited soil-plant system. We calibrated our own
land surface model (LSM) mirroring CLM v5 (Oleson et al., 2018) (section S6 of the Supplement) to the surface energy budget

235 and gross primary productivity (GPP) data at the Ameriflux Metolius ponderosa pine site in Oregon, USA (US-Me2 (Irvine et al., 2008)) for May-August 2013-2014. We use the calibrated LSM to (i) explore the spectrum of transport-limitation in a realistic system, (ii) quantify errors incurred by selecting β over a PHM, and (iii) develop and test a new 'dynamic β' that approximates the behaviors of the PHM with two additional parameters to the original β function.
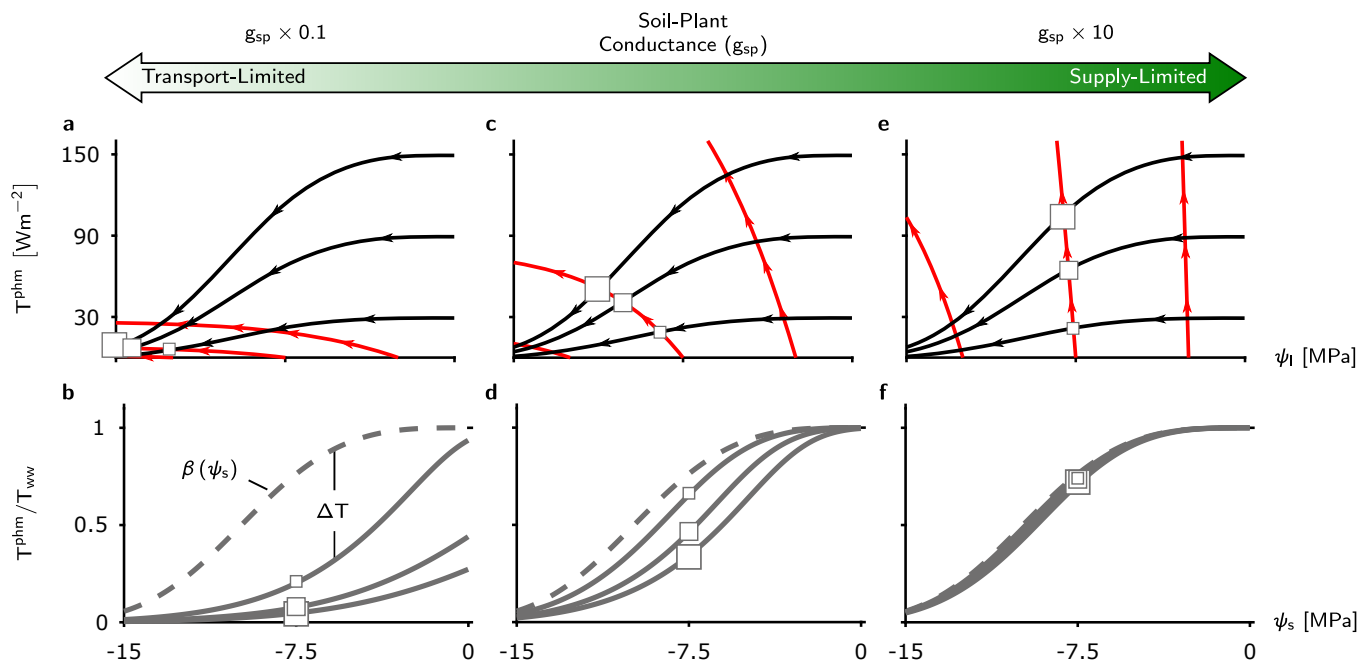
Figure 3. Transport-limitation spectrum observed in complex PHM formulation. **a,c,e,** Supply-demand curves for three values of soil-plant conductance, g_{sp}, using the more complex PHM formulation. Panel **c** is based on calibrated parameters from the US-Me2 Ameriflux site containing mature ponderosa pines that were determined for the LSM analysis in this paper. Panels **a** and **e** contains the calibrated g_{sp} multiplied by 0.1 and 10, respectively. The supply lines (red) are shown at ψ_s equal to 0, -7.5, and -15 MPa and demand lines (black) are shown at T_{ww} equal to 30, 90, and 150 W m^{-2}. The PHM solution for ψ_s at -7.5 MPa is shown by the squares with size corresponding to T_{ww} magnitude. **b,d,f,** The relative transpiration for the PHM (solid) in panels **a**, **c**, and **e** and the infinitely conductive β solution (dashed line).

Our calibrated LSM uses a more complex formulation of the PHM common to TBMs (Bonan et al., 2014; Kennedy et al.,
240 2019; Williams et al., 2001; Xu et al., 2016; Christoffersen et al., 2016) and ecohydrological models (Sperry et al., 1998; Manzoni et al., 2014) that partitions the soil-plant-atmosphere continuum into soil-to-xylem, xylem-to-leaf, and leaf-to-atmosphere segments, and uses nonlinear (e.g., sigmoidal or Weibull) functions to represent downregulation of segment-specific conductances (Eq. 6-13). This added complexity does not affect the the spectrum of transport-limitation found in the minimalist PHM, shown for the calibrated LSM in an analogous supply-demand framework in Fig. 3. Two main points are worth reiterating. First,
245 soil-plant conductance (g_{sp}) controls whether the soil-plant system is supply-limited (high g_{sp}; Fig. 3e-f) or transport-limited (low g_{sp}; Fig. 3a-b) due to non-negligible water potential differences ($\Delta\psi$), resulting in large differences between PHMs and

β (high ΔT) at intermediate ψ_s values (Fig. 3b,d). Second, for a transport-limited system, ΔT increases with higher variability in T_{ww}. To elaborate on this second point, we note that the plotted β function is shown in this case as an upper bound of transport-limited behavior (as $g_{sp} \to \infty$). However, in practice, β is an empirical model; depending on how the modeler

250   chooses to fit the β function, it could exist anywhere within the range of the PHM downregulation envelope. Therefore, we must emphasize that the larger range of T_{ww} results in a greater range of downregulation behaviors from the PHM (Fig. 3b), making a single β increasingly inadequate for capturing the range of behaviors within this downregulation envelope. The consistency in the results based on the minimalist and the more complex PHM suggests that the divergence between PHMs and β in transport-limited systems is not contingent on the linear or nonlinear forms of supply or demand lines, but rather on the

255   existence of a finite conductance itself. Furthermore, these results strongly support the need to use two independent variables, ψ_s and T_{ww} (rather than only ψ_s in β), to capture the coupled effects of soil water stress and atmospheric moisture demand on transpiration downregulation when soil-plant systems are transport-limited.

    In light of these findings, we have developed a new 'dynamic β' (β_{dyn}) that has an additional functional dependence on T_{ww} (Eq. 16) and compared it against four other downregulation schemes in this LSM analysis. Thus, the LSM was run using

260   a total of five different transpiration downregulation schemes: 1) well-watered (no downregulation), 2) single β (β_s), 3) β separately applied to sunlit and shaded leaf areas (β_{2L}), 4) β_{dyn}, and 5) PHM. The LSM with PHM scheme was calibrated to the Ameriflux data while the β schemes were each fit to the calibrated relative transpiration outputs (T^{phm}/T_{ww}) that vary with both ψ_s and T_{ww} as previously suggested (Fig. 4a-b). We refer the reader to the Sect. 2.3 for calibration and fitting details.

    The median diurnal evapotranspiration (ET) from each LSM is compared to the Ameriflux data for early and late summer

265   2013-2014 (Fig. 4c-d). During early summer, all models perform similarly due to high soil moisture and minimal downregulation (Fig. 4c). During late summer, soil moisture declines (Fig. S1 of the Supplement), and differences between downregulation schemes emerge. The PHM and β_{dyn} schemes fit the ET observations the best, while β_{2L}, β_s, and well-watered schemes over-predict ET (Fig. 4d). The sources of bias for the static β schemes are illustrated by plotting the reduction in absolute percent bias between the β_s and PHM schemes (Fig. 4e) for a range of soil (represented by volumetric soil water content,

270   θ_s [m^3 water m^{-3} soil]) and atmospheric moisture conditions (represented by T_{ww}). The PHM provides substantial percent bias reduction relative to the static β_s scheme under soil water stress ($\theta_s < 0.2$) for above- and below-average T_{ww} values ($T_{ww} \approx 120\,\mathrm{W\,m^{-2}}$). This result is true for both static β schemes (β_s and β_{2L}) because they are fit to the average T_{ww} at each ψ_s over the simulation period (Fig. 4a-b). Therefore, as T_{ww} becomes higher (lower) than the average, these static schemes will overpredict (underpredict) transpiration. The PHM also improves performance during wetter soil conditions ($\theta_s > 0.2$)

275   with high T_{ww}—which do not represent typical 'drought' conditions—suggesting that PHMs are more appropriate than β for representing transpiration downregulation caused by large soil-plant potential differences ($\Delta\psi$) under high atmospheric moisture demand. Lastly, the near average T_{ww} conditions lead to β providing enhanced performance, which can be explained by underlying biases in the calibrated parameter estimates (see Fig. S10 of the Supplement).

    Notably, the β_{dyn} downregulation scheme replicates the performance of the PHM scheme by adding a single dimension

280   of T_{ww} to the original β scheme. The difference in performance between PHM and β_{dyn} schemes is minimal in terms of percent change in bias across all environmental conditions (Fig. 4f), median diurnal variations (Fig. 4a-b), and cumulative
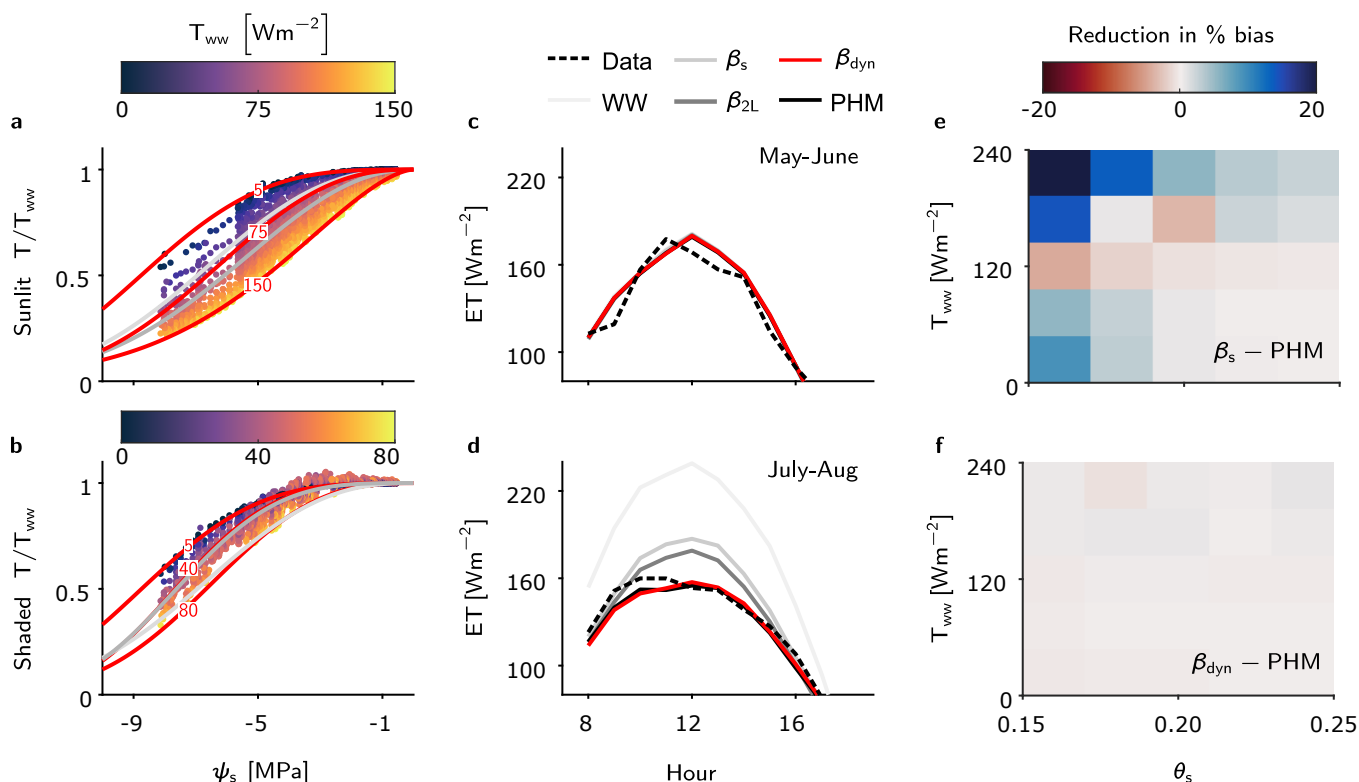
Figure 4. LSM evapotranspiration estimates improved by PHM and new 'dynamic β'. **a-b**, Fits of the β_s, β_{2L}, and β_{dyn} schemes to the relative transpiration outputs from the calibrated PHM scheme for the sunlit (**a**) and shaded big leaf (**b**) of the LSM (see Methods). Note that only three of the infinite family of β_{dyn} curves are shown for illustration. Full fitting details of these three schemes are available in section S2 of the Supplement. **c-d**, The median diurnal ET estimates for the LSM with five transpiration downregulation schemes compared to Ameriflux observations at the US-Me2 site for early (**c**) and late summer (**d**). The dual source LSM calculates ET as the sum of sunlit and shaded big leaf transpiration and ground evaporation. Note: β_{dyn} (red) is overlying PHM (black) results as they are essentially the same. **e-f**, Reduction in absolute percent bias between the β_s and PHM schemes (**e**) and β_{dyn} and PHM schemes (**f**) in terms of atmospheric moisture demand (represented by T_{ww}) and soil water status (represented by θ_s). In both plots, blue indicates PHM improvement over the selected β scheme.

flux errors (Table S1 of the Supplement). Therefore, this additional dependence on T_{ww} is key to simulating the coupled effects of atmospheric moisture demand and soil water stress in PHMs and accurately modeling transpiration downregulation in transport-limited systems.

285 ## 4   Discussion and Outlook

The spectrum of transport-limited transpiration highlighted in this work explains why many TBMs that use β to represent transpiration downregulation struggle to predict water, energy, and carbon fluxes under soil water stress (Sitch et al., 2008;

Powell et al., 2013; Medlyn et al., 2016; Ukkola et al., 2016; Restrepo-Coupe et al., 2017; Trugman et al., 2018) and why
implementing PHMs has led to performance improvements (Kennedy et al., 2019; Anderegg and Venturas, 2020; Eller et al.,
290 2020; Sabot et al., 2020). A transport-limited system, characterized by finite soil-plant conductance, leads to a non-negligible
water potential difference between the soil and the leaf. It is only when the soil-plant conductance becomes infinite (and the
system becomes supply-limited) that leaf water potential approximates soil water potential, and transpiration arises as an inde-
pendent function of soil water supply and atmospheric moisture demand. These are assumptions inherent to the empirical β and
explains why β cannot capture the coupled effects of soil water stress and atmospheric moisture demand. The implications of
295 continued use of β will vary by site. Ecosystems with soil or plant hydraulic properties resistant to flow (e.g., xeric ecosystems,
tall trees, species with low xylem conductivity or roots that hydraulically disconnects from the soil during drought) will have
large biases depending on the range of soil water availability and atmospheric moisture demand (T_{ww}) observed at the site
(Fig. 2d and 3b). These errors will not be confined to drought periods, and will also occur during wetter soil conditions (low
soil water stress) when atmospheric moisture demand is high (Fig. 2 and Fig. 4e). This is a crucial point, given that ecosystems
300 are projected to experience diverging degrees of VPD stress and soil water stress in the future (Novick et al., 2016). On the
other hand, for supply-limited systems (e.g., riparian vegetation, irrigated crops, or groundwater-dependent ecosystems), β
may adequately capture transpiration dynamics. Therefore, identifying the combinations of soil parameters and plant hydraulic
traits that define transport- or supply-limited systems is an important future step for locating areas around the globe susceptible
to prediction error. Our initial estimates indicate a value of soil-plant conductance around $10^3 \, \mathrm{W \, m^{-2} \, MPa^{-1}}$ may act as a
305 rough threshold for transport-limitation (see section S3 of the Supplement).

The recognition that a 'dynamic β' model can replicate the complexity of a PHM with half the parameters and direct
computation (see section S2.2 of the Supplement), simply by adding a dependence on atmospheric moisture demand to the
β function, provides a useful pathway for overcoming both the limitations of β and the parametric uncertainties of PHMs
(Paschalis et al., 2020; Anderegg and Venturas, 2020). The inadequacies of the static β have been noted since its inception.
310 Feddes et al. (1978), who introduced the first β, mentioned β's dependence on atmospheric moisture demand based on field
data (Denmead and Shaw, 1962; Yang and de Jong, 1972) and early plant hydraulic theory (Gardner, 1960). Unfortunately,
there have been only a few attempts to rectify these inadequacies in the modeling community, short of implementing a full
PHM. For example, Feddes and Raats (2004) updated their original β model to vary the water potential at incipient stomatal
closure linearly with atmospheric moisture demand, which has been adopted in the field scale SWAP model (Kroes et al., 2017),
315 while the Ecosystem Demography-2 model (Medvigy et al., 2009) uses a sigmoidal function for transpiration downregulation
that contains the ratio of soil water supply to evaporative demand. Within many TBMs and hydrological models, a 'dynamic
β' could easily replace the original β by allowing existing fixed parameters to vary with T_{ww} (already calculated in many
transpiration downregulation schemes). This would offer a physically-informed alternative to PHMs, with a simpler calibration
process. In addition to improving TBM performances, 'dynamic β' also has the potential to aid in remote sensing retrievals and
320 indirect inferences of land surface fluxes. Currently, the state-of-the-art ECOSTRESS satellite provides global ET estimates
based on a modified Priestley-Taylor formulation that uses a β function to downregulate ET under soil water stress (Fisher
et al., 2020). These satellite products could easily implement the 'dynamic β' formulation to correct biases for many transport-

limited ecosystems. These potential applications rely on formalizing the relationship between the 'dynamic β' parameters and their dependence on T_{ww}. Further work will focus on linking these relationships to measurable soil properties, plant hydraulic

325   traits, and atmospheric feedbacks.

Code availability.   The MATLAB code used for the LSM analysis in Sect. 3.3 will be made available upon acceptance of this manuscript. The LSM description is available in section S6 of the Supplement.

Author contributions.   X.F. and S.T. conceived the idea; B.P.S and X.F. designed the research; B.P.S. performed the research; B.P.S. and X.F. wrote the paper; and S.T. contributed to refining results and revising the paper.

330   *Competing interests.*   The authors declare no competing interests.

Acknowledgements.   The authors have no acknowledgements to make.

References

Anderegg, W. R., Wolf, A., Arango-Velez, A., Choat, B., Chmura, D. J., Jansen, S., Kolb, T., Li, S., Meinzer, F., Pita, P., Resco de Dios, V., Sperry, J. S., Wolfe, B. T., and Pacala, S.: Plant water potential improves prediction of empirical stomatal models, PLoS ONE, 12, 1–17,
335   https://doi.org/10.1371/journal.pone.0185481, 2017.

Anderegg, W. R. L.: Minireview Spatial and temporal variation in plant hydraulic traits and their relevance for climate change impacts on vegetation, New Phytologist, 205, 1008–1014, https://doi.org/10.1111/nph.12907, www.newphytologist.com, 2015.

Anderegg, W. R. L. and Venturas, M. D.: Plant hydraulics play a critical role in Earth system fluxes, New Phytologist, N/A, 4, https://doi.org/10.1111/nph.16548, http://doi.wiley.com/10.1111/nph.16548, 2020.

340   Bonan, G.: Climate Change and Terrestrial Ecosystem Modeling, Cambridge University Press, https://doi.org/10.1017/9781107339217, https://www.cambridge.org/core/product/identifier/9781107339217/type/book, 2019.

Bonan, G. B., Williams, M., Fisher, R. A., and Oleson, K. W.: Modeling stomatal conductance in the earth system: linking leaf water-use efficiency and water transport along the soil–plant–atmosphere continuum, Geoscientific Model Development, 7, 2193–2222, https://doi.org/10.5194/gmd-7-2193-2014, https://www.geosci-model-dev.net/7/2193/2014/, 2014.

345   Buckley, T. N. and Mott, K. A.: Modelling stomatal conductance in response to environmental factors, Plant, Cell and Environment, 36, 1691–1699, https://doi.org/10.1111/pce.12140, https://onlinelibrary.wiley.com/doi/pdf/10.1111/pce.12140, 2013.

Christoffersen, B. O., Gloor, M., Fauset, S., Fyllas, N. M., Galbraith, D. R., Baker, T. R., Kruijt, B., Rowland, L., Fisher, R. A., Binks, O. J., Sevanto, S., Xu, C., Jansen, S., Choat, B., Mencuccini, M., McDowell, N. G., and Meir, P.: Linking hydraulic traits to tropical forest function in a size-structured and trait-driven model (TFS v.1-Hydro), Geoscientific Model Development, 9, 4227–4255,
350   https://doi.org/10.5194/gmd-9-4227-2016, https://www.geosci-model-dev.net/9/4227/2016/, 2016.

Clapp, R. B. and Hornberger, G. M.: Empirical equations for some soil hydraulic properties, Water Resources Research, 14, 601–604, https://doi.org/10.1029/WR014i004p00601, http://doi.wiley.com/10.1029/WR014i004p00601, 1978.

Cowan, I. R.: Transport of Water in the Soil-Plant-Atmosphere System, Tech. Rep. 1, 1965.

Daly, E., Porporato, A., Rodriguez-Iturbe, I., Daly, E., Porporato, A., and Rodriguez-Iturbe, I.: Coupled Dynamics of Photosynthe-
355   sis, Transpiration, and Soil Water Balance. Part I: Upscaling from Hourly to Daily Level, Journal of Hydrometeorology, 5, 546–558, https://doi.org/10.1175/1525-7541(2004)005<0546:CDOPTA>2.0.CO;2, http://journals.ametsoc.org/doi/abs/10.1175/1525-7541%282004%29005%3C0546%3ACDOPTA%3E2.0.CO%3B2, 2004.

Damour, G., Simonneau, T., Cochard, H., and Urban, L.: An overview of models of stomatal conductance at the leaf level, Plant, Cell and Environment, 33, 1419–1438, https://doi.org/10.1111/j.1365-3040.2010.02181.x, 2010.

360   Denmead, O. T. and Shaw, R. H.: Availability of Soil Water to Plants as Affected by Soil Moisture Content and Meteorological Conditions 1, Agronomy Journal, 54, 385–390, https://doi.org/10.2134/agronj1962.00021962005400050005x, http://doi.wiley.com/10.2134/agronj1962.00021962005400050005x, 1962.

Eller, C. B., Rowland, L., Mencuccini, M., Rosas, T., Williams, K., Harper, A., Medlyn, B. E., Wagner, Y., Klein, T., Teodoro, G. S., Oliveira, R. S., Matos, I. S., Rosado, B. H. P., Fuchs, K., Wohlfahrt, G., Montagnani, L., Meir, P., Sitch, S., and Cox, P. M.: Stomatal optimization
365   based on xylem hydraulics (SOX) improves land surface model simulation of vegetation responses to climate, New Phytologist, N/A, 1–16, https://doi.org/10.1111/nph.16419, https://onlinelibrary.wiley.com/doi/abs/10.1111/nph.16419, 2020.

Fatichi, S., Pappas, C., and Ivanov, V. Y.: Modeling plant-water interactions: an ecohydrological overview from the cell to the global scale, Wiley Interdisciplinary Reviews: Water, 3, 327–368, https://doi.org/10.1002/wat2.1125, http://doi.wiley.com/10.1002/wat2.1125, 2016.

Feddes, R. A. and Raats, P. C.: Parameterizing the soil - water - plant root system, in: Unsaturated-zone modeling: Progress, challenges and applications, chap. 4, pp. 95–141, Kluwer Academic Publishers, Dordrecht, 2004.

Feddes, R. A., Kowalik, P. J., and Zaradny, H.: Simulation of field water use and crop yield. Simulation monographs, Halsted Press, Wageningen, 1978.

Feng, X.: Marching in step: The importance of matching model complexity to data availability in terrestrial biosphere models, Global Change Biology, 26, 3190–3192, https://doi.org/10.1111/gcb.15090, https://onlinelibrary.wiley.com/doi/abs/10.1111/gcb.15090, 2020.

Feng, X., Ackerly, D. D., Dawson, T. E., Manzoni, S., Skelton, R. P., Vico, G., and Thompson, S. E.: The ecohydrological context of drought and classification of plant responses, Ecology Letters, N/A, 14, https://doi.org/10.1111/ele.13139, 2018.

Fisher, J. B., Lee, B., Purdy, A. J., Halverson, G. H., Dohlen, M. B., Cawse-Nicholson, K., Wang, A., Anderson, R. G., Aragon, B., Arain, M. A., Baldocchi, D. D., Baker, J. M., Barral, H., Bernacchi, C. J., Bernhofer, C., Biraud, S. C., Bohrer, G., Brunsell, N., Cappelaere, B., Castro-Contreras, S., Chun, J., Conrad, B. J., Cremonese, E., Demarty, J., Desai, A. R., De Ligne, A., Foltýnová, L., Goulden, M. L., Griffis, T. J., Grünwald, T., Johnson, M. S., Kang, M., Kelbe, D., Kowalska, N., Lim, J.-H., Maïnassara, I., Mccabe, M. F., Missik, J. E. C., Mohanty, B. P., Moore, C. E., Morillas, L., Morrison, R., Munger, J. W., Posse, G., Richardson, A. D., Russell, E. S., Ryu, Y., Sanchez-Azofeifa, A., Schmidt, M., Schwartz, E., Sharp, I., Šigut, L., Tang, Y., Hulley, G., Anderson, M., Hain, C., French, A., Wood, E., Hook, S., Fisher, J. B., Lee, B., Purdy, A. J., Halverson, G. H., Dohlen, M. B., and Fisher, A. L.: ECOSTRESS: NASA's Next Generation Mission to Measure Evapotranspiration From the International Space Station, Water Resources Research, 56, https://doi.org/10.1029/2019WR026058, https://doi.org/, 2020.

Gardner, W. R.: Dynamic aspects of water availability to plants, Soil Science, 89, 63–73, https://doi.org/10.1097/00010694-196002000-00001, 1960.

Goudriaan, J. and Laar, H. H. v.: Modelling potential crop growth processes : textbook with exercises, https://doi.org/10.1007/978-94-011-0750-1, 1994.

Irvine, J., Law, B. E., Martin, J. G., and Vickers, D.: Interannual variation in soil CO2 efflux and the response of root respiration to climate and canopy gas exchange in mature ponderosa pine, Global Change Biology, 14, 2848–2859, https://doi.org/10.1111/j.1365-2486.2008.01682.x, 2008.

Jarvis, P.: The interpretation of the variations in leaf water potential and stomatal conductance found in canopies in the field, Tech. rep., 1976.

Katul, G. G., Oren, R., Manzoni, S., Higgins, C., and Parlange, M. B.: Evapotranspiration: A process driving mass transport and energy exchange in the soil-plant-atmosphere-climate system, https://doi.org/10.1029/2011RG000366, 2012.

Kennedy, D., Swenson, S., Oleson, K. W., Lawrence, D. M., Fisher, R., Lola da Costa, A. C., and Gentine, P.: Implementing Plant Hydraulics in the Community Land Model, Version 5, Journal of Advances in Modeling Earth Systems, 11, 485–513, https://doi.org/10.1029/2018MS001500, http://doi.wiley.com/10.1029/2018MS001500, 2019.

Klein, T.: The variability of stomatal sensitivity to leaf water potential across tree species indicates a continuum between isohydric and anisohydric behaviours, Functional Ecology, 28, 1313–1320, https://doi.org/10.1111/1365-2435.12289, http://doi.wiley.com/10.1111/1365-2435.12289, 2014.

Kowalczyk, E. A., Wang, Y. P., Law, R. M., Davies, H. L., Mcgregor, J. L., and Abramowitz, G.: The CSIRO Atmosphere Biosphere Land Exchange (CABLE) model for use in climate models and as an offline model, Tech. rep., http://www.cmar.csiro.au/e-print/open/kowalczykea_2006a.pdf, 2006.

405 Kroes, J. G., van Dam, J., Bartholomeus, R., Groenendijk, P., Heinen, M., Hendriks, R., Mulder, H., Supit, I., and van Walsum, P.: SWAP version 4: Theory description and user manual, Tech. rep., Wageningen Environmental Research, Wageningen, https://doi.org/ISSN 1566-7197, 2017.

Lin, C., Gentine, P., Huang, Y., Guan, K., Kimm, H., and Zhou, S.: Diel ecosystem conductance response to vapor pressure deficit is suboptimal and independent of soil moisture, Agricultural and Forest Meteorology, 250-251, 24–34,
410 https://doi.org/10.1016/J.AGRFORMET.2017.12.078, https://www.sciencedirect.com/science/article/pii/S0168192317304884, 2018.

Liu, Y., Kumar, M., Katul, G. G., Feng, X., and Konings, A. G.: Plant hydraulics accentuates the effect of atmospheric moisture stress on transpiration, Nature Climate Change, 10, 691–695, https://doi.org/10.1038/s41558-020-0781-5, https://doi.org/10.1038/s41558-020-0781-5, 2020.

Manzoni, S., Vico, G., Katul, G., Palmroth, S., and Porporato, A.: Optimal plant water-use strategies under stochastic rainfall, Water Re-
415 sources Research, 50, 1–16, https://doi.org/10.1002/2014WR015375, 2014.

McAdam, S. A. M. and Brodribb, T. J.: Linking Turgor with ABA Biosynthesis: Implications for Stomatal Responses to Vapor Pressure Deficit across Land Plants., Plant physiology, 171, 2008–16, https://doi.org/10.1104/pp.16.00380, http://www.ncbi.nlm.nih.gov/pubmed/27208264, 2016.

Medlyn, B. E., Duursma, R. A., Eamus, D., Ellsworth, D. S., Prentice, I. C., Barton, C. V. M., Crous, K. Y., De Angelis, P., FREEMAN, M.,
420 and WINGATE, L.: Reconciling the optimal and empirical approaches to modelling stomatal conductance, Global Change Biology, 17, 2134–2144, https://doi.org/10.1111/j.1365-2486.2010.02375.x, http://doi.wiley.com/10.1111/j.1365-2486.2010.02375.x, 2011.

Medlyn, B. E., De Kauwe, M. G., Zaehle, S., Walker, A. P., Duursma, R. A., Luus, K., Mishurov, M., Pak, B., Smith, B., Wang, Y.-P., Yang, X., Crous, K. Y., Drake, J. E., Gimeno, T. E., Macdonald, C. A., Norby, R. J., Power, S. A., Tjoelker, M. G., and Ellsworth, D. S.: Using models to guide field experiments: a priori predictions for the CO 2 response of a nutrient- and water-limited native Eucalypt woodland,
425 Global Change Biology, 22, 2834–2851, https://doi.org/10.1111/gcb.13268, http://doi.wiley.com/10.1111/gcb.13268, 2016.

Medvigy, D., Wofsy, S. C., Munger, J. W., Hollinger, D. Y., and Moorcroft, P. R.: Mechanistic scaling of ecosystem function and dynamics in space and time: Ecosystem Demography model version 2, Journal of Geophysical Research: Biogeosciences, 114, G01 002, https://doi.org/10.1029/2008JG000812, http://doi.wiley.com/10.1029/2008JG000812, 2009.

Mencuccini, M., Manzoni, S., and Christoffersen, B. O.: Modelling water fluxes in plants: from tissues to biosphere, New Phytologist,
430 https://doi.org/10.1111/nph.15681, 2019.

Novick, K. A., Ficklin, D. L., Stoy, P. C., Williams, C. A., Bohrer, G., Oishi, A. C., Papuga, S. A., Blanken, P. D., Noormets, A., Sulman, B. N., Scott, R. L., Wang, L., and Phillips, R. P.: The increasing importance of atmospheric demand for ecosystem water and carbon fluxes, Nature Climate Change, 6, 1023–1027, https://doi.org/10.1038/nclimate3114, 2016.

Oleson, K. W., Lead, D. M. L., Bonan, G. B., Drewniak, B., Huang, M., Koven, C. D., Levis, S., Li, F., Riley, W. J., Subin, Z. M., Swen-
435 son, S. C., Thornton, P. E., Bozbiyik, A., Fisher, R., Heald, C. L., Kluzek, E., Lamarque, J.-F., Lawrence, P. J., Leung, L. R., Lipscomb, W., Muszala, S., Ricciuto, D. M., Sacks, W., Sun, Y., Tang, J., and Yang, Z.-L.: Technical Description of the version 5.0 of the Community Land Model (CLM), Tech. rep., http://www.cesm.ucar.edu/models/cesm2/land/CLM50_Tech_Note.pdfhttp://library.ucar.edu/research/publish-technote, 2018.

Pammenter, N. W. and Willigen, C. V.: A mathematical and statistical analysis of the curves illustrating vulnerability of xylem to cavitation,
440 in: Tree Physiology, https://doi.org/10.1093/treephys/18.8-9.589, 1998.

Paschalis, A., Fatichi, S., Zscheischler, J., Ciais, P., Bahn, M., Boysen, L., Chang, J., De Kauwe, M., Estiarte, M., Goll, D., Hanson, P. J., Harper, A. B., Hou, E., Kigel, J., Knapp, A. K., Larsen, K. S., Li, W., Lienert, S., Luo, Y., Meir, P., Nabel, J. E., Ogaya, R.,

Parolari, A. J., Peng, C., Peñuelas, J., Pongratz, J., Rambal, S., Schmidt, I. K., Shi, H., Sternberg, M., Tian, H., Tschumi, E., Ukkola, A., Vicca, S., Viovy, N., Wang, Y. P., Wang, Z., Williams, K., Wu, D., and Zhu, Q.: Rainfall manipulation experiments as simulated by terrestrial biosphere models: Where do we stand?, Global Change Biology, 26, 3336–3355, https://doi.org/10.1111/gcb.15024, https://onlinelibrary-wiley-com.ezp1.lib.umn.edu/doi/full/10.1111/gcb.15024https://onlinelibrary-wiley-com.ezp1.lib.umn.edu/doi/abs/10.1111/gcb.15024https://onlinelibrary-wiley-com.ezp1.lib.umn.edu/doi/10.1111/gcb.15024, 2020.

Powell, T. L., Galbraith, D. R., Christoffersen, B. O., Harper, A., Imbuzeiro, H. M., Rowland, L., Almeida, S., Brando, P. M., da Costa, A. C. L., Costa, M. H., Levine, N. M., Malhi, Y., Saleska, S. R., Sotta, E., Williams, M., Meir, P., and Moorcroft, P. R.: Confronting model predictions of carbon fluxes with measurements of Amazon forests subjected to experimental drought, New Phytologist, 200, 350–365, https://doi.org/10.1111/nph.12390, 2013.

Prentice, I. C., Liang, X., Medlyn, B. E., and Wang, Y.-P.: Reliable, robust and realistic: the three R's of next-generation land-surface modelling, Atmospheric Chemistry and Physics, 15, 5987–6005, https://doi.org/10.5194/acp-15-5987-2015, https://www.atmos-chem-phys.net/15/5987/2015/, 2015.

Razavi, S., Sheikholeslami, R., Gupta, H. V., and Haghnegahdar, A.: VARS-TOOL: A toolbox for comprehensive, efficient, and robust sensitivity and uncertainty analysis, Environmental Modelling and Software, 112, 95–107, https://doi.org/10.1016/j.envsoft.2018.10.005, 2019.

Restrepo-Coupe, N., Levine, N. M., Christoffersen, B. O., Albert, L. P., Wu, J., Costa, M. H., Galbraith, D., Imbuzeiro, H., Martins, G., da Araujo, A. C., Malhi, Y. S., Zeng, X., Moorcroft, P., and Saleska, S. R.: Do dynamic global vegetation models capture the seasonality of carbon fluxes in the Amazon basin? A data-model intercomparison, Global Change Biology, 23, 191–208, https://doi.org/10.1111/gcb.13442, http://doi.wiley.com/10.1111/gcb.13442, 2017.

Rogers, A., Medlyn, B. E., Dukes, J. S., Bonan, G., von Caemmerer, S., Dietze, M. C., Kattge, J., Leakey, A. D. B., Mercado, L. M., Niinemets, , Prentice, I. C., Serbin, S. P., Sitch, S., Way, D. A., and Zaehle, S.: A roadmap for improving the representation of photosynthesis in Earth system models, New Phytologist, 213, 22–42, https://doi.org/10.1111/nph.14283, http://doi.wiley.com/10.1111/nph.14283, 2017.

Sabot, M. E. B., De Kauwe, M. G., Pitman, A. J., Medlyn, B. E., Verhoef, A., Ukkola, A. M., and Abramowitz, G.: Plant profit maximization improves predictions of European forest responses to drought, New Phytologist, N/A, 1–18, https://doi.org/10.1111/nph.16376, https://onlinelibrary.wiley.com/doi/abs/10.1111/nph.16376, 2020.

Schwarz, P. A., Law, B. E., Williams, M., Irvine, J., Kurpius, M., and Moore, D.: Climatic versus biotic constraints on carbon and water fluxes in seasonally drought-affected ponderosa pine ecosystems, Global Biogeochemical Cycles, 18, 1–17, https://doi.org/10.1029/2004GB002234, 2004.

Sitch, S., Huntingford, C., Gedney, N., Levy, P. E., Lomas, M., Piao, S. L., Betts, R., Ciais, P., Cox, P. M., Friedlingstein, P., Jones, C. D., Prentice, I. C., and Woodward, F. I.: Evaluation of the terrestrial carbon cycle, future plant geography and climate-carbon cycle feedbacks using five Dynamic Global Vegetation Models (DGVMs), Global Change Biology, 14, 2015–2039, https://doi.org/10.1111/j.1365-2486.2008.01626.x, http://doi.wiley.com/10.1111/j.1365-2486.2008.01626.x, 2008.

Sperry, J. S. and Love, D. M.: What plant hydraulics can tell us about responses to climate-change droughts, New Phytologist, 207, 14–27, https://doi.org/10.1111/nph.13354, http://doi.wiley.com/10.1111/nph.13354, 2015.

Sperry, J. S., Adler, F. R., Campbell, G. S., and Comstock, J. P.: Limitation of plant water use by rhizosphere and xylem conductance: Results from a model, Plant, Cell and Environment, 21, 347–359, https://doi.org/10.1046/j.1365-3040.1998.00287.x, 1998.

Trugman, A. T., Medvigy, D., Mankin, J. S., and Anderegg, W. R.: Soil Moisture Stress as a Major Driver of Carbon Cycle Uncertainty, Geophysical Research Letters, 45, 6495–6503, https://doi.org/10.1029/2018GL078131, 2018.

Ukkola, A. M., De Kauwe, M. G., Pitman, A. J., Best, M. J., Abramowitz, G., Haverd, V., Decker, M., and Haughton, N.: Land surface models systematically overestimate the intensity, duration and magnitude of seasonal-scale evaporative droughts, Environmental Research Letters, 11, 104 012, https://doi.org/10.1088/1748-9326/11/10/104012, https://iopscience.iop.org/article/10.1088/1748-9326/11/10/104012https://iopscience.iop.org/article/10.1088/1748-9326/11/10/104012/meta, 2016.

485 Ukkola, A. M., Haughton, N., De Kauwe, M. G., Abramowitz, G., and Pitman, A. J.: FluxnetLSM R package (v1.0): a community tool for processing FLUXNET data for use in land surface modelling, Geosci. Model Dev, 10, 3379–3390, https://doi.org/10.5194/gmd-10-3379-2017, https://doi.org/10.5194/gmd-10-3379-2017, 2017.

Verhoef, A. and Egea, G.: Modeling plant transpiration under limited soil water: Comparison of different plant and soil hydraulic parameterizations and preliminary implications for their use in land surface models, Agricultural and Forest Meteorology, 191, 22–32,

490 https://doi.org/10.1016/J.AGRFORMET.2014.02.009, https://www.sciencedirect.com/science/article/pii/S0168192314000483, 2014.

Williams, M., Law, B. E., Anthoni, P. M., and Unsworth, M. H.: Use of a simulation model and ecosystem flux data to examine carbon-water interactions in ponderosa pine, Tree Physiology, 21, 287–298, https://doi.org/10.1093/treephys/21.5.287, 2001.

Xu, X., Medvigy, D., Powers, J. S., Becknell, J. M., and Guan, K.: Diversity in plant hydraulic traits explains seasonal and inter-annual variations of vegetation dynamics in seasonally dry tropical forests, New Phytologist, 212, 80–95, https://doi.org/10.1111/nph.14009,

495 http://doi.wiley.com/10.1111/nph.14009, 2016.

Yang, S. J. and de Jong, E.: Effect of Aerial Environment and Soil Water Potential on the Transpiration and Energy Status of Water in Wheat Plants 1, Agronomy Journal, 64, 574–578, https://doi.org/10.2134/agronj1972.00021962006400050006x, http://doi.wiley.com/10.2134/agronj1972.00021962006400050006x, 1972.

Zhou, S., Duursma, R. A., Medlyn, B. E., Kelly, J. W., and Prentice, I. C.: How should we model plant responses to drought?

500 An analysis of stomatal and non-stomatal responses to water stress, Agricultural and Forest Meteorology, 182-183, 204–214, https://doi.org/10.1016/J.AGRFORMET.2013.05.009, https://www.sciencedirect.com/science/article/pii/S0168192313001263, 2013.